

DOI: 10.15825/1995-1191-2022-4-94-108

TISSUE-ENGINEERED VASCULAR PATCHES: COMPARATIVE CHARACTERISTICS AND PRECLINICAL TEST RESULTS IN A SHEEP MODEL

L.V. Antonova¹, A.V. Mironov¹, A.R. Shabaev¹, V.N. Silnikov², E.O. Krivkina¹,
V.G. Matveeva¹, E.A. Velikanova¹, E.A. Senokosova¹, M.Yu. Khanova¹, V.V. Sevostyanova¹,
T.V. Glushkova¹, R.A. Mukhamadiyarov¹, L.S. Barbarash¹

¹ Research Institute for Complex Issues of Cardiovascular Diseases, Kemerovo, Russian Federation

² Institute of Chemical Biology and Fundamental Medicine, Novosibirsk, Russian Federation

Carotid endarterectomy (CEA) with patch angioplasty is the most effective treatment for carotid artery stenosis. However, the use of existing vascular patches is often associated with thrombosis, restenosis, calcification and other complications. **Objective:** to develop biodegradable patches for arterial reconstruction, containing vascular endothelial growth factor (VEGF) or arginyl-glycyl-aspartic acid (RGD), and comparatively evaluate their biocompatibility and efficacy in in vitro experiments and during preclinical trials in large laboratory animal models. **Materials and methods.** Biodegradable patches, made from a mixture of poly(3-hydroxybutyrate-co-3-hydroxyvalerate) (PHBV) and poly(ϵ -caprolactone) (PCL), were fabricated by electrospinning and modified with VEGF or the peptide sequence RGD in different configurations. In in vitro experiments, the surface structure, physicochemical and hemocompatibility properties were evaluated. In in vivo experiments, we evaluated the effectiveness of the developed vascular patches for 6 months after implantation into the carotid artery of 12 sheep. The quality of remodeling was assessed using histological and immunofluorescence studies of explanted specimens. **Results.** The PHBV/PCL/VEGF patches had physicochemical characteristics closer to those of native vessels and their biofunctionalization method resulted in the smallest drop in strength characteristics compared with their unmodified PHBV/PCL counterparts. Modification with RGD peptides reduced the strength of the polymer patches by a factor of 2 without affecting their stress-strain behavior. Incorporation of VEGF into polymer fibers reduced platelet aggregation upon contact with the surface of the PHBV/PCL/VEGF patches and did not increase erythrocyte hemolysis. At month 6 of implantation into the carotid artery of sheep, the PHBV/PCL/VEGF patches formed a complete newly formed vascular tissue without signs of associated inflammation and calcification. This indicates the high efficiency of the VEGF incorporated into the patch. In contrast, the patches modified with different configurations of RGD peptides combined the presence of neointimal hyperplasia and chronic granulomatous inflammation present in the patch wall and developed during bioresorption of the polymer scaffold. **Conclusion.** PHBV/PCL/VEGF patches have better biocompatibility and are more suitable for vascular wall reconstruction than PHBV/PCL/RGD patches.

Keywords: vascular patch, tissue engineering, poly(3-hydroxybutyrate-co-3-hydroxyvalerate), poly(ϵ -caprolactone), vascular endothelial growth factor, RGD peptides, biodegradable polymers, endothelialization.

INTRODUCTION

Cardiovascular diseases are the major cause of death and disability globally. Atherosclerosis remains the leading cause, which results in the formation and enlargement of atheromatous plaque, disrupting blood flow to the tissues. Atherosclerotic internal carotid artery (ICA), leading to carotid stenosis, causes 10–15% of all strokes [1].

CEA and carotid stenting are the main surgical treatments for carotid stenosis [2]. In turn, CEA is the gold standard for surgical treatment and prevention of acute stroke, demonstrating significant advantage in asymp-

tomatic and symptomatic patients with high degree of ICA stenosis [2]. However, the presence of prolonged plaques makes it difficult to perform this procedure by the standard and most frequently used method – eversion carotid endarterectomy (eCEA). Therefore, surgeons are forced to resort to closure of the arteriotomy access using a patch [3, 4].

To date, a large number of papers with comparative results of carotid artery reconstruction using biological and synthetic patches have been published. Ren S. and colleagues found no difference in mortality, stroke and restenosis rates in CEA with venous patch versus

synthetic patch material, or in CEA with Dacron patch versus polytetrafluoroethylene (PTFE) patch [5]. However, mean operative time was significantly longer with PTFE or Dacron patch due to prolonged hemostasis for suture line bleeding, whereas in the case of carotid angioplasty with biological material (xeno-pericardial), a significant reduction in suture line bleeding was noted. At the same time, the use of synthetic patches is associated with infection and thrombosis, while xeno-pericardial patch is associated with a high risk of calcification [5].

A recent meta-analysis of eight randomized control trials assessing the effectiveness of PTFE, Dacron and bovine pericardium patches, found no significant differences in a wide range of complications, including stenosis in the long-term period [6].

According to Russian authors, the incidence of perioperative strokes in the group with arterial plasty by xenopericardium was 1.5%, and ischemic strokes in the early postoperative period was 0.26%; these complications were not identified in the group with PTFE patches [7]. In the long-term follow-up, the incidence of hemodynamically significant ICA restenosis over 70% was higher when PTFE patches were used (31.2%) than when xeno-pericardial flaps were used (9.8%).

Tissue-engineered vascular patches can help avoid the problems encountered with existing materials by restoring the implant site's own tissues. To achieve such a result, the biodegradable matrix should have high biocompatibility, ensure migration of cells into the thickness of the material, their proliferation and differentiation. At the same time, the need for rapid formation of endothelial monolayer from autologous cells on the inner surface of the patches required finding ways to stimulate this process. A number of works have shown that VEGF has a great potential in stimulating endothelialization and vascular regeneration based on tissue-engineered matrices [8, 9]. Being the main angiogenic growth factor, VEGF stimulates migration and survival of endothelial cells as well as recruitment of progenitor cells from the bloodstream [10, 11].

Peptides with the RGD sequence are present in most extracellular matrix proteins. The RGD sequence can be considered a common integrin-binding motif [12]. Nevertheless, the affinity for endothelial cells makes RGDs ideal agents for modifying tissue-engineered constructs contacting with blood and requiring early surface endothelialization. Both peptide sequences obtained during extraction from natural material and artificially synthesized ones can be used for modification. The latter have a number of advantages: the risk of immune response and infection that can be associated with an insufficient degree of purification of the natural material, is reduced. When comparing the functional properties of natural RGD-containing proteins and their artificial counterparts, the latter proved to be more effective [13].

Thus, the currently used patches cannot fully meet the needs of vascular surgery, due to, among other reasons, the lack of functional activity in terms of formation of new vascular tissue on their base. Therefore, the issue of selecting a patch that would meet all the requirements necessary to reduce the risk of complications in the early and late postoperative periods remains relevant.

The **objective** of the study is to develop biodegradable patches for arterial reconstruction containing VEGF or RGD, and comparatively evaluate their biocompatibility and efficacy in *in vitro* experiments and in preclinical trials in large laboratory animal models.

MATERIALS AND METHODS

1. Fabrication of biodegradable patches with VEGF

Polymeric matrices were fabricated by emulsion electrospinning on a Nanon-01A machine (MECC CO, Japan) according to the protocol described earlier [14]. A mixture of 5% PHBV (Sigma-Aldrich, USA) and 10% PCL (Sigma-Aldrich, USA) in trichloromethane in a 1 : 2 ratio was prepared. Then, VEGF (Sigma-Aldrich, USA) diluted in a saline solution to a 10 µg/mL concentration was added to the polymer solution in a 20 : 1 ratio. Emulsion electrospinning was performed under the following parameters: 20 kV voltage, 0.5 mL/h feed rate, 200 rpm manifold rotation speed, 15 cm distance to the collector, and 22G needle. A metal pin with a diameter of 8.0 mm was used as the manifold. Before removal from the pin, the matrix was cut lengthwise and removed with peeling movements.

Unmodified patches, made by electrospinning from PHBV/PCL polymer mixture in trichloromethane in a 1 : 2 ratio, were used as the control group. Used as the comparison group was xeno-pericardial flap KemPeriplas-Neo (NeoCor, Russia), which is currently actively used in the clinic as a vascular patch during carotid endarterectomy.

2. Assessment of VEGF distribution during incorporation into biodegradable PHBV/PCL patches

To assess the expected distribution pattern of VEGF injected into the polymer solution in a liquid phase, an analog technique was used to incorporate fluorochrome-labeled bovine serum albumin (BSA) into the PHBV/PCL matrix. For this purpose, PHBV/PCL solution in chloroform was mixed with a BSA-Texas Red[®] solution (Invitrogen, USA) in phosphate-buffered saline (10 µg/mL) in a 20 : 1 ratio. Electrospinning was performed at 20 kV, a feed rate of 0.5 mL/h, and a microscopy slide was used as the manifold. The obtained specimens were examined on an Axio Imager A1 microscope (Carl Zeiss, Germany) using a BP 546/12 – FT 580 – LP 590 light filter.

3. Fabrication of biodegradable patches with RGD and detection of arginine-rich peptides on the patch surface

Polymer matrices were fabricated by electrospinning on a Nanon-01A machine (MECC CO, Japan) according to the protocol described previously [15].

Before modification with RGD peptides, oil and dust residues were removed from the surface of PHBV/PCL matrices using a 1 : 1 mixture of 2-propanol and water with further washing with deionized water. To activate the polymer surfaces, the matrices were treated with 10% ethylenediamine (EDA) dissolved in 2-propanol at 37 °C for 1 hour. The matrices were then washed thoroughly with 0.3% Tween-20 solution in deionized water and air dried.

Then, in accordance with the previously described technique, primary modification of the patch surface with amino groups was performed using 4,7,10-trioxal-1,13-tridecanediamine (Sigma-Aldrich, USA) as a linker group [16]. The PHBV/PCL patch surface was further modified using RGD containing peptides produced by NanoTech-S (Russia): RGDK (P1), AhRGD (P2), c[RGDFK] (P3) [16]. Thus, 3 varieties of RGD-modified patches were obtained: PHBV/PCL/P1, PHBV/PCL/P2, and PHBV/PCL/P3.

The method for determining the presence of arginine-rich peptides was performed according to the Saccucci method [17]. Arginine/aspartic acid solution (1 mg/mL in deionized water) was used as the positive control. The reference values were taken from Sedaghati et al. [18]. Orange-red staining of the sample indicated the presence of the guanidinium group characteristic of arginine.

4. Assessment of the surface structure of vascular patches before and after implantation into the carotid artery of sheep

Before implantation, specimens of PHBV/PCL, PHBV/PCL/VEGF, PHBV/PCL/RGD, and KemPeriplas-Neo patches 0.5 × 0.5 cm in size were subjected to gold-palladium sputtering to obtain a 15 nm coating using an EM ACE200 sputtering system (Leica Mikrosysteme GmbH, Austria) and studied on a scanning electron microscope S-3400N (Hitachi, Japan) under high vacuum conditions at an accelerating voltage of 10 kV.

5. Physical and mechanical testing of vascular patches

Specimens of unmodified and modified patches (n = 6 in each group) were cut longitudinally. The mechanical properties of the PHBV/PCL/VEGF and PHBV/PCL/RGD vascular patches were evaluated under uniaxial tension conditions on a universal testing machine (Zwick/Roell, Germany) according to the procedure described earlier [14]. Strength and stress-strain properties were

evaluated using a transducer with a nominal force of 50 N and a crosshead travel speed of 10 mm/min during the test. The strength of the material was evaluated by the maximum tensile stress (MPa). Elasticity and stiffness of the material were evaluated by relative elongation corrected for specimen fracture behavior (%) and Young's modulus (MPa). To measure the thickness of the specimens, a thickness gauge with a ±0.01 mm error limit (measuring force not more than 1.5 N) was used. The carotid artery of a sheep and the human internal thoracic artery (A. mammaria) were used as controls. Human A. mammaria segments were taken during coronary artery bypass surgery from patients who signed an informed consent for the material to be taken. Xeno-pericardial flap KemPeriplas-Neo (NeoCor, Russia) and unmodified PHBV/PCL specimens were used as comparison groups. The specimens were cut out longitudinally.

6. Assessment of hemocompatibility of the patches

To assess the hemocompatibility of the developed patches, we studied erythrocyte hemolysis and platelet aggregation after fresh citrate blood and platelet-rich plasma had come in contact with the patch surfaces. The studies were performed according to the methods described in [19].

7. Implantation of biodegradable vascular patches into the carotid artery of sheep

A series of experiments was carried out on Edilbay sheep, weighing 42–45 kg. All the animals were non-pregnant females. The animals were operated on sequentially. When performing experimental studies, we were guided by the requirements of order No. 1179 of the USSR Ministry of Health, dated October 10, 1983, and order No. 267 of the Russian Ministry of Health dated June 19, 2003 "Rules for handling experimental animals", principles of the European Convention (Strasbourg, 1986) and the World Medical Association Declaration of Helsinki about humane treatment of animals (1996). The work was approved by the local ethics committee of the Research Institute for Complex Issues of Cardiovascular Diseases (protocol No. of September 11, 2018).

Biodegradable vascular patches PHBV/PCL/VEGF (n = 3), PHBV/PCL/P1 (n = 3), PHBV/PCL/P2 (n = 3), and PHBV/PCL/P1 (n = 3) were implanted into the carotid artery of sheep. Patch size was 40.0 × 4.0 mm. Follow-up after implantation lasted for 6 months.

Anesthesia: Premedication: Xylazine (Xylanit) 0.05–0.25 mL per 10 kg of animal weight + atropine 1 mg IM. Induction anesthesia: 5–7 mg of propofol per 1 kg of animal weight; within 90 seconds after that, atracurium besylate (Ridelat) is administered at IV dose of 0.5–0.6 mg/kg. Tracheal intubation with a 9.0 endotracheal tube. Anesthesia maintenance: Sevoran 2–4 vol%,

Ridelat was administered by continuous infusion at a rate of 0.3–0.6 mg/kg/h.

Monitoring: blood pressure (BP), heart rate (HR), blood oxygen saturation (SpO₂). Artificial ventilation: Respiratory rate (RR) 12–15/min, PEEP 7–9 mbar, tidal volume (TV) 6–8 ml/kg, FiO₂ – 40–60%.

Main stage: Carotid artery access; systemic heparinization – 5000 IU IV; carotid artery clamping, longitudinal carotid incision 40 mm long, implantation of 40 × 4 mm vascular patches with separate knotty sutures using Prolene 6/0 thread (Ethicon, USA). Standard protocol for prevention of air embolism and triggering of blood flow; wound closure with Vicril 2.0 suture (Ethicon, USA); suture treatment with BF glue, enoxaparin sodium subcutaneously 4000 anti-Ha IU/0.4 ml; extubation.

Intraoperative drug administration: infusion of 0.9% NaCl 500 ml – IV drip; Axetine (cefuroxime) 1.5 g – IV drip.

Postoperative medical management: antibiotic therapy (Axetine (cefuroxime) 1.5 g – IM/m twice daily + enoxaparin sodium subcutaneously 4000 anti-Ha IU/0.4 ml for 5 days. With proven vascular patency with implanted patches: clopidogrel 75 mg orally once daily + sodium heparin 5000 IU subcutaneously twice daily).

Postoperative ultrasound screening of the patched vessels patency was performed after 1 and 5 days, then once every 3 months up to the expected date of animal withdrawal from experiment.

8. Histological study of explanted specimens of biodegradable vascular patches

The explanted vascular patch specimens with surrounding carotid artery sections were divided into 2 parts. One part was frozen at –140 °C for subsequent immunofluorescence study. The second part was used for histological study using H&E, Van Gieson and Alizarin red S stains, which were described earlier [14].

After each type of staining, all specimens were examined by light microscopy using an AXIO Imager A1 microscope (Carl Zeiss, Germany) at 50×, 100×, and 200× magnifications.

9. Immunofluorescence study of explanted specimens of biodegradable vascular patches

From frozen sections of explanted vascular patches, serial 8 μm thick cryosections were made using a cryotome (Thermo Scientific, USA). The preparations were fixed in 4% paraformaldehyde solution for 10 minutes. Before staining for intracellular markers, the sections were permeabilized with Triton-X100 solution (Sigma-Aldrich, USA) for 15 minutes. They were then stained with primary antibodies in the following combinations: rabbit anti-CD31 antibodies (Abcam, UK) and mouse anti-alpha smooth muscle actin antibody (α-SMA, Ab-

cam, UK); rabbit anti-von Willebrand factor (vWF, Abcam, UK); rabbit anti-collagen type IV antibody (Abcam, UK) and mouse anti-collagen type I antibody (Abcam, UK); rabbit anti-collagen type III antibody (Novus Biologicals, USA).

The sections were incubated with antibodies overnight at 4 °C, then with goat secondary antibodies to rabbit IgG conjugated with Alexa Fluor 488-conjugated (Thermo Fisher, USA), and goat antibodies to mouse IgG conjugated with Alexa Fluor 555-conjugated (Thermo Fisher Scientific, USA) for 1 hour at room temperature. At all stages of staining, phosphate-buffered saline with the addition of 0.1% Tween (Sigma-Aldrich, USA) was used for intermediate washing of the sections.

To remove autofluorescence, the sections were treated with Autofluorescence Eliminator Reagent (Millipore, USA) according to the manufacturer's procedure. Nuclei were contrasted using DAPI staining (10 μg/mL, Sigma-Aldrich, USA) for 30 minutes. Stained preparations were incubated under a coverslip using ProLong mounting medium (Thermo Fisher, USA). The preparations were analyzed using a scanning laser microscope LSM 700 confocal microscope (Carl Zeiss, Germany).

10. Statistical data processing

Data were analyzed using Prism (Graph Pad Software). Normality of distribution was assessed by Kolmogorov–Smirnov test. Mann–Whitney U test was used to compare two independent groups. When comparing three or more independent groups, the nonparametric Kruskal–Wallis H test was used; when the groups were compared in pairs, the Dunn's test was used. Differences were considered significant at significance level $p < 0.05$. Data are presented as median and 25th and 75th percentiles of Me (25%; 75%).

RESULTS

To manufacture biodegradable vascular patches with VEGF, emulsion electrospinning was used, which can be used to introduce bioactive molecules into a polymer fiber composition, which can then be controlled and stably released from the matrix in the process of its resorption [20–22].

To assess the expected distribution pattern of VEGF injected into the polymer solution in a liquid phase, we performed an analog experiment with BSA labeled with Texas Red and incorporated into the PHBV/PCL matrix. Fig. 1 (a, b) shows that aqueous domains with BSA-Texas Red are evenly distributed in the thickness of polymer fiber along its entire length. At the same time, the fiber structure was not violated.

Modification of PHBV/PCL biodegradable patches made by electrospinning with RGD peptides was performed to biofunctionalize the inner surface of patches in order to attract and fully adhere mature and progenitor

endothelial cells and form an endothelial monolayer. Tripeptide RGD was chosen as a modifying agent because it is a cell adhesion site and is present in the structure of most natural extracellular matrix proteins. Three configurations of RGD were obtained by chemical synthesis: RGDK (linear configuration of the molecule, Arg-Gly-Asp-Lys sequence), AhRGD (linear configuration of the molecule, Ah-Arg-Gly-Asp sequence and c[RGDFK] (cyclic configuration of the molecule, c[Arg-Gly-Asp-Phe-Lys] sequence).

L-lysine, which contains two amino groups (-NH₂) and one carboxyl group (-COOH), and is used for surface modification of various materials to improve their adhesive properties and biocompatibility, was used in synthesis of linear RGDK molecule [23]. During the synthesis of linear molecule AhRGD, a synthetic analogue of L-lysine, aminocaproic acid (Ah), was added to the basic adhesive tripeptide RGD. Aminocaproic acid is used in medical practice as an antifibrinolytic drug because of its ability to inhibit fibrinolysis. Cyclic configurations of RGD with constant geometry of the molecule, according to literature data, are able to demonstrate maximum affinity to cellular receptors in comparison with their linear analogues [24]. Therefore, the cyclic RGD peptide c[RGDFK] was the third type of RGD used for surface modification of vascular patches.

Previously, we proved that the linker length significantly affects the availability of RGD peptides for

cellular receptors; therefore, in this work, extended hydrophilic linker 4,7,10-trioxa-1,13-tridecanediamine [16] was used for aminolysis of the PHBV/PCL matrix surface. RGD peptide was injected using a cross-linking reagent. The presence of peptides on the polymer surface was confirmed using the Sakaguchi test for the presence of arginine (Fig. 1, c) [17]. After covalent attachment of RGD peptide, the light-yellow staining did not disappear after washing the PHBV/PCL/RGD polymer patch specimens. The light-yellow staining of unmodified PHBV/PCL patches that did not contain RGD on their surface disappeared when washed (Fig. 1, c).

Structural features of patches

Scanning electron microscopy (SEM) of the surface of biodegradable vascular patches was compared with xeno-pericardial patch KemPeriplas-Neo (Neocor, Kemerovo), which is actively used in the clinic during endarterectomy of internal carotid arteries. The preservation of the native architectonics of the xeno-pericardial flap, which consisted in relief due to the tortuosity of collagen fibers, was shown. High density of collagen fibers caused the absence of pores.

SEM of polymer patch surface before implantation into the vascular bed showed that all biodegradable specimens, both unmodified and those containing VEGF or RGD, had a highly porous structure and consisted

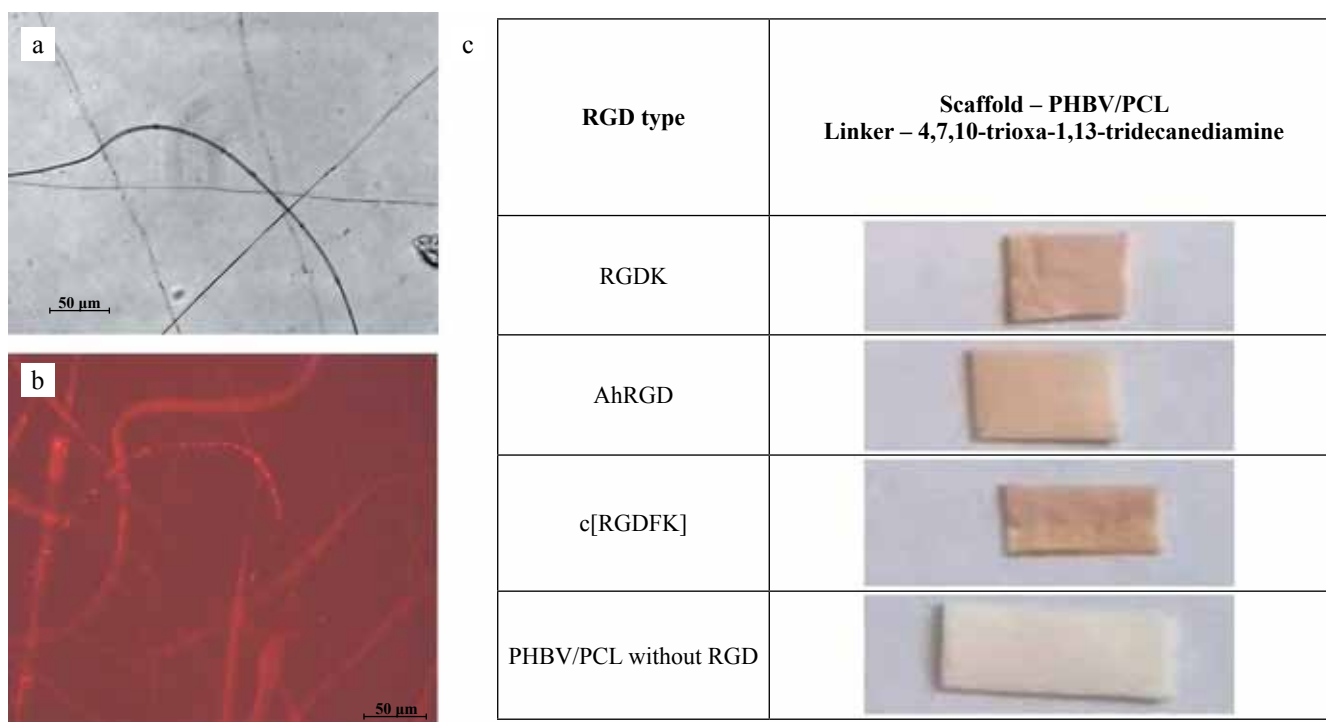


Fig. 1. Test results confirming the incorporation/attachment of bioactive peptides into the structure/to the matrix surface. a, b, incorporation of fluorescein-labeled BSA into the PHBV/PCL scaffold during emulsion electrospinning: a, light microscopy (400× magnification); b, fluorescence microscopy (400× magnification); c, results of RGD peptide detection on the surface of PHBV/PCL scaffold obtained using Sakaguchi test

of micro-sized multidirectional fibers (Fig. 2). The PHBV/PCL/VEGF fibers were $1.47 \pm 0.67 \mu\text{m}$ in diameter, which was 1.8-fold smaller than for PHBV/PCL/RGD and unmodified PHBV/PCL ($2.64 \pm 1.14 \mu\text{m}$; $p < 0.05$), which is associated with the use of emulsion electrospinning to make patches with VEGF.

Additional modification using RGD did not change the architectonics of the patch surface (Fig. 2).

Mechanical properties of patches

Mechanical test results demonstrate that the strength of the PHBV/PCL/VEGF patches was 1.7-fold lower than that of the PHBV/PCL patches that did not contain VEGF ($p < 0.05$) (Table 1). However, the strength of PHBV/PCL/VEGF patches was fully consistent with that of the human internal thoracic artery and 1.9-fold greater than that of sheep carotid artery. The force applied to the

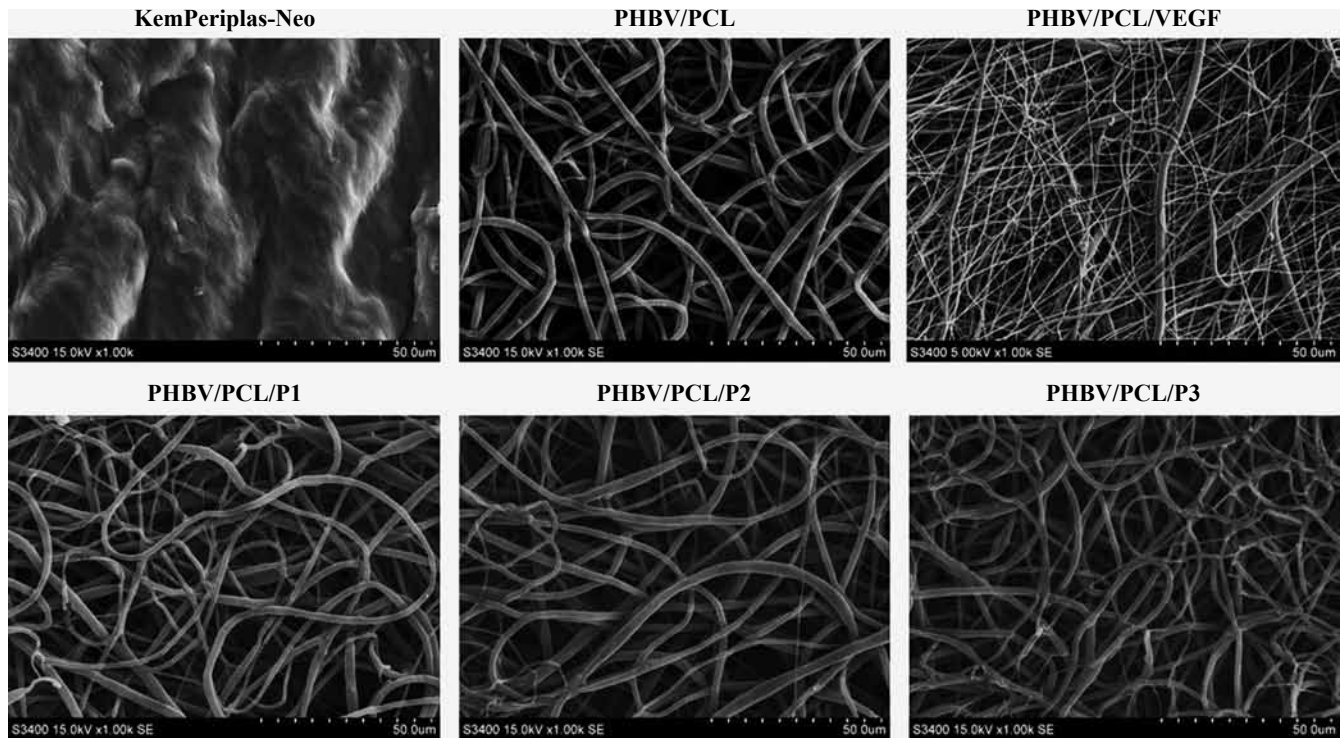


Fig. 2. Morphology of the inner surface of vascular patches PHBV/PCL, PHBV/PCL/VEGF, PHBV/PCL/RGD and xenopericardial patch KemPeriplas-Neo. Scanning electron microscopy, 1000 \times magnification

Table 1

Physicomechanical properties of PHBV/PCL polymer patches before and after VEGF incorporation or RGD modification in comparison with the KemPeriplas-Neo flap and a. mammaria. Data are presented as Me (25–75%)

| | Voltage (MPa) | F_{\max} (N) | Relative elongation (%) | Young's modulus (MPa) | Sample thickness (mm) |
|----------------------|----------------------------|--------------------------|-----------------------------|---------------------------|-----------------------|
| PHBV/PCL | 3.9 (2.88–4.5)*/**■ | 3.0 (2.59–3.3)*/**■ | 102.7 (79.37–106.3)*/**■ | 21.8 (19.2–25.2)*/**■ | 0.4 (0.35–0.5)* |
| PHBV/PCL/VEGF | 2.25 (2.14–2.6)**■ | 1.97 (1.82–2.3)*■ | 81.83 (77.0–103.4)*/** | 16.9 (15.5–17.5)*/**■ | 0.43 (0.4–0.5)* |
| PHBV/PCL /RGD | 1.2 (1.12–1.3)*■ | 1.3 (1.2–1.4)* | 102.6 (80.38–144.1)*/**■ | 21.8 (20.15–23.9)*/**■ | 0.5 (0.49–0.5)* |
| Sheep carotid artery | 1.2 (1.06–1.9)* | 1.01 (0.88–1.42) | 158.5* (126.0–169.5) | 0.49* (0.39–0.66) | 0.25 (0.23–0.3) |
| Human a. mammaria | 2.48 (1.36–3.25)** | 0.92 (0.59–1.72) | 29.72 (23.51–39.62)** | 2.42 (1.87–3.19)** | 0.27■ (0.24–0.3) |
| KemPeriplas-Neo | 10.06 (9.12–21.38)*/**■ | 15.4 (12.6–26.2)*/**■ | 64.96 (61.08–72.6)*/**■ | 1.11 (1.02–1.34)■ | 0.69 (0.63–0.7)* |

*, $p < 0.05$ versus A. mammaria; **, $p < 0.05$ versus sheep carotid artery; #, $p < 0.05$ versus PHBV/PCL; ■, $p < 0.05$ versus KemPeriplas-Neo.

specimen before it began to break was 2.1-fold higher in the PHBV/PCL/VEGF patches than in a. mammaria, 1.9-fold higher than in the sheep carotid artery, and 1.5-fold lower than in the PHBV/PCL specimens ($p < 0.05$). The differences in performance between PHBV/PCL/VEGF and PHBV/PCL may be related to the fact that aqueous domains with the growth factor within the fiber create additional points that are unable to withstand load. These are points where polymer filament is more likely to damage, leading to reduced strength and less force required to break.

We also did not observe a significant change in relative elongation in polymer patches after injection of the growth factor compared to unmodified counterparts (Table 1). Introduction of VEGF reduced the stiffness of the polymer matrix by 1.3-fold ($p < 0.05$).

A preliminary study of the physical and mechanical properties of biodegradable patches, whose surface was modified with various RGD-containing peptides, found no significant intergroup differences. Therefore, to further compare the physical and mechanical parameters of modified patches with unmodified ones, xeno-pericardial flap and native human and sheep vessels, all specimens of patches modified with RGD peptides were combined into one group – PHBCV/PCL/RGD.

It was found that the strength of PHBV/PCL/RGD was identical to that of sheep carotid, but was 2-fold lower than that of a. mammaria ($p < 0.05$). The force exerted on the specimen before destruction in PHBV/PCL/RGD patches did not differ from that of native vessels but was 1.5-fold lower than in PHBV/PCL/VEGF patches and 2.3-fold lower than in unmodified PHBV/PCL, ($p < 0.05$), (Table 1). The relative elongation of all biodegra-

dable patches did not differ among themselves but was, on average, 3.2-fold higher than that of a. mammaria, 1.5-fold higher than that of xeno-pericardial patches, and 1.7-fold lower than that of sheep carotid, ($p < 0.05$). The Young’s modulus of unmodified patches and PHBV/PCL/RGD patches was 44-fold higher than that of sheep carotid artery, 9-fold higher than that of a. mammaria, 19.6-fold higher than that of xeno-pericardial flap, and 1.3-fold higher than that of the PHBV/PCL/VEGF specimens ($p < 0.05$).

All biodegradable vascular patches, regardless of the modification method, were significantly less strong and stiffer than the xeno-pericardial flap, as indicated by such indicators as stress, force and Young’s modulus (Table 1). However, KemPeriplas-Neo differed significantly in its physical and mechanical characteristics from a. mammaria and sheep carotid artery as well (Table 1). Thus, the stress and force applied to the specimen before its destruction was 4-fold and 16.7-fold higher in xeno-pericardium than in a. mammaria, and 8.4-fold and 15.2-fold higher than in sheep carotid artery ($p < 0.05$). At the same time, the Young’s modulus of KemPeriplas-Neo was 2.6-fold lower than that of internal thoracic artery and 2.3-fold lower than that of the sheep carotid artery, although the xeno-pericardial flap was 2.6-fold thicker than the wall thickness of the native vessels ($p < 0.05$).

Thus, the PHBV/PCL/VEGF patches had physico-mechanical characteristics closer to those of native vessels; their biofunctionalization technique resulted in the least drop in strength characteristics relative to the unmodified PHBV/PCL counterparts. Modification of RGD reduced the strength of polymer patches without affecting their stress-strain behavior.

Table 2

Degree of hemolysis and maximum aggregation of human blood platelets after contact with PHBV/PCL polymer patches before and after VEGF incorporation or RGD modification in comparison with xeno-pericardial flap KemPeriplas-Neo

| Sample type | Degree of RBC hemolysis (%) | Maximum platelet aggregation (%) |
|-----------------------------|-----------------------------|----------------------------------|
| | Me (25–75%) | Me (25–75%) |
| PHBV/PCL | 0.5 (0–1.01)* | 87.23 (83.95–89.84)*■ |
| PHBV/PCL/VEGF | 0.5 (0–1.01)* | 81.35 (81.01–88.51)* |
| PHBV/PCL/RGD | 0.72 (0–0.72)* | 86.15 (82.24–87.43)*■ |
| KemPeriplas-Neo | 2.12 (0.9–3.95) | 93.32 (84.24–96.42)■ |
| Intact platelet-rich plasma | – | 74.65 (72.45–75.31) |

*, $p < 0.05$ versus KemPeriplas-Neo flap; ■, $p < 0.05$ versus intact platelet-rich plasma.

Outcomes of hemolysis

The degree of hemolysis after contact with the VEGF-, RGD- modified patch, and unmodified PHBV/PCL patches was 0.5%, 0.72%, and 0.5%, respectively, without statistically significant differences (Table 2), thus confirming them to be highly hemocompatible [25].

The level of hemolysis after contact with the surface of the KemPeriplas-Neo flap was 3-fold higher than that after contact of red blood cells with the surface of biodegradable patches, but did not go beyond the acceptable values [25].

Outcomes of platelet aggregation

The results of the study showed that platelet aggregation activity upon contact with the surface of the PHBV/PCL and PHBV/PCL/RGD patches was 1.2-fold greater than that of intact platelet-rich plasma (PRP), ($p < 0.05$), (Table 2). Maximum platelet aggregation after contact with PHBV/PCL/VEGF specimens was the lowest among all biodegradable specimens.

The contact of platelets with the surface of the KemPeriplas-Neo flap revealed the most significant increase in the maximum aggregation up to 93.32 (84.24; 96.42) %, which was 1.3-fold higher than the maximum aggregation of platelets from intact PRP, ($p < 0.05$). There was no significant difference between the xenogeneic pericardial flap and PHBV/PCL patches before and after VEGF or RGD modification (Table 2).

Therefore, the PHBV/PCL/VEGF and PHBV/PCL/RGD polymer patches caused a lower degree of hemolysis and platelet aggregation than the KemPeriplas-Neo flap.

Outcomes of implantation of biodegradable vascular patches into sheep carotid artery

We previously studied the biocompatibility and efficacy of patches with VEGF and various RGD configurations in a comparative aspect with unmodified PHBV/PCL patches and KemPeriplas-Neo xeno-pericardial flaps in a rat model [14, 16]. Biodegradable patches demonstrated ease of implantation. Throughout the experiment, no bleeding and or violation of the integrity of the implants were noted. It was proved that after 12 months of implantation, vessels that were prosthethized with PHBV/PCL/VEGF had 100% patency and no neointimal hyperplasia. A mature endothelial monolayer on the inner surface of PHBV/PCL/VEGF patches was fully formed after 3 months, whereas on the unmodified PHBV/PCL patches, only after 12 months. Remodeling of the patches was accompanied by repopulation by cells with the formation of an extracellular matrix.

With long-term implantation of PHBV/PCL/RGD patches into the aorta of rats, it has been proven that elements of new vascular tissue can be formed on their basis: both migration of cellular elements into the thickness of the patch and formation of neointimal lining with an endothelial layer from the side of vessel lumen occur, especially when patches are modified with peptides P3 and P1 [16].

PHBV/PCL polymer patches modified with VEGF or RGD experienced slight calcinosis at 12 months of implantation in rat aorta. At the same time, PHBV/PCL/VEGF and PHBV/PCL/P1 patches demonstrated maximum resistance to calcification.

KemPeriplas-Neo xeno-pericardial flaps, on their basis, were unable to support the development of new vascular tissue and endothelial layer, and were prone to calcification already after one month of implantation into rat aorta. After 12 months of implantation of KemPeriplas-Neo flaps, massive deposition of crystalline calcium in 100% of the implanted flaps and delamination of their wall, which led to shape deformation, were detected. Also after 12 months of implantation, 50% of the xeno-pericardial flaps showed neointimal hyperplasia, whose thickness was almost 3-fold greater than that of rat aortic wall [14, 16].

Tests on the rat model confirmed the low efficiency and biocompatibility of xeno-pericardial flaps and insufficient ability of unmodified PHBV/PCL to form a new vascular tissue on its base. Therefore, only PHBV/PCL/VEGF, PHBV/PCL/P1, PHBV/PCL/P2, and PHBV/PCL/P3 patches were included in the protocol of preclinical trials in sheep.

The sheep model was used to implant the developed vascular patches, which is optimal for in vivo testing of cardiovascular implants, as it is suitable for worst-case modeling due to the increased tendency of their vessels to calcification and blood to hypercoagulation. Therefore, the use of the sheep model allows for the most rigorous testing of vascular prostheses, including their degeneration in vivo [26–30]. In addition, sheep are considered an optimal animal model for assessment of growth, permeability, endothelialization, thromboresistance and post-implant imaging of products for cardiovascular surgery.

It is known that the high porosity of tissue-engineered matrix and nanosized fibers in its structure can provide cell migration inside the matrix and early endothelialization of its surface due to the similarity of the surface structure to that of natural extracellular matrix and a larger area of interaction between cells and artificial matrix [31–33]. In its turn, effective infiltration of cells into the thickness of the porous material promotes its better integration with native tissues at the implantation site.

Two sheep (with implanted PHBV/PCL/P1 and PHBV/PCL/P2 patches) did not survive to the expected date of withdrawal from experiment, dying at 14 days due to formation of massive paravascular hematomas around the operated vessels. Most likely, this was due to micro-damage in the patch wall in response to pulse wave after implantation, since no bleeding from the suture areas was detected immediately after implantation and hemostasis was achieved within 2 minutes.

All sheep with implanted PHBV/PCL/VEGF and PHBV/PCL/P3 patches survived to the expected withdrawal date. During six months of follow-up, the vessels with implanted patches maintained their patency. No aneurysmal dilatation of the vessels in the implanted patch site was detected. However, all vessels with RGD patches showed increased blood flow velocity, which may be an indirect reflection of vessel lumen narrowing.

According to the results of morphological examination (histological study and scanning electron microscopy) of the patches with vascular endothelial growth factor, we can see that after 6 months of implantation into sheep carotid artery, a complete three-layer newly-formed vascular tissue was formed on the basis of these patches (Fig. 3).

Thin neointima, covered by a layer of endothelium-like cells on the vessel lumen side, lined the entire inner surface of the patches. The bulk of the neointima consisted of smooth muscle cells. Next came the patch itself. There were processes of visible biodegradation of the

polymer matrix accompanied by disruption in its integrity, visible only by specimen microscopy. The PHBV/PCL/VEGF patch was filled with cellular elements (ma-

crophages, fibroblast-like and smooth muscle cells, few foreign-body giant cells), permeated with bundles of collagen fibers. There were vasa vasorum in the patch

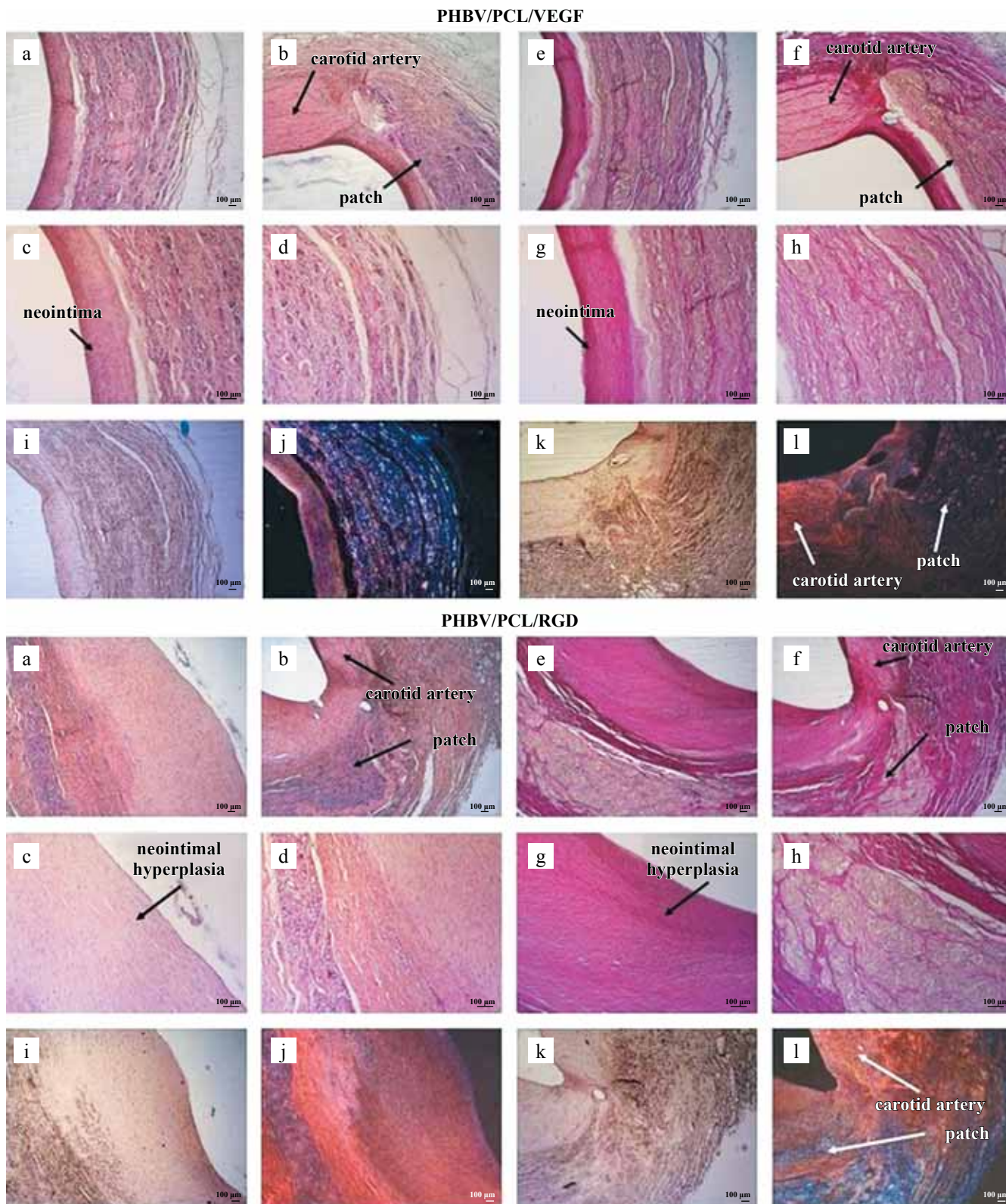


Fig. 3. Results of histological examination of PHBV/PCL/VEGF and PHBV/PCL/RGD vascular patches at month 6 of implantation into sheep carotid artery: a–d, H&E stain; e–h, Van Gieson’s stain; i–l, Alizarin Red S stain (i, k, light microscopy; j, l, fluorescent microscopy); a, e, i, j, central part of the patch; b, f, k, l, junction of the patch and carotid artery in the anastomosis zone; c, e, inner and middle layer of the patch wall; d, h, middle and outer layer of the patch wall. a, b, e, f, i–l, 50× magnification; c, d, g, h, 100× magnification

thickness. External layer of the patches contained all structural elements characteristic of natural adventitial layer: collagen fibers, fibroblasts and fibrocytes, single foreign-body giant cells, lymphoid follicles and vasa vasorum. There were no signs of calcification (Fig. 3).

When studying the histological pattern of explanted specimens of PHBV/PCL/RGD patches, we obtained a similar picture – all the specimens had neointimal hyperplasia (Fig. 3). The neointima thickness corresponded to the thickness of the wall of the patch itself. The neointima surface facing the vessel lumen was covered by a cell monolayer. The walls of the patches were partially resorbed and contained a moderate number of foreign-body multinucleated giant cells. Macrophages, smooth muscle and fibroblast-like cells, and bundles of collagen fibers were also present in the patch walls; vasa vasorum were formed (Fig. 3).

Histological examination (Alizarin Red S staining) showed that there was no calcium deposition in the explanted PHBV/PCL/RGD patches (Fig. 3).

The large extent of the implanted patches made it possible to perform slices during immunofluorescence study such that the carotid artery wall, into which the patch was implanted, was opposite the patch (Fig. 4). This arrangement led to better visualization of the similarity of the new vascular tissue formed on the basis of

the patches within 6 months of their implantation with the native sheep carotid artery. The neointima formed on the inner surface of the PHBV/PCL/VEGF patches was proved to consist of smooth muscle cells, as evidenced by the presence of alpha actin in the cells (Fig. 4). On the vessel lumen side, the neointima was lined by mature CD31+ endothelial cells secreting von Willebrand factor vWF+ throughout its entire length (Fig. 4). Type IV collagen formed a basal membrane on which endothelial cells were located and was detected in large numbers both in the patch wall thickness and in the sheep carotid artery wall. Type III collagen was formed throughout the patch thickness with a predominant concentration at the basal membrane and in the neointima (Fig. 4).

Thus, on the basis of the biodegradable VEGF patch, after 6 months of its implantation into sheep carotid arteries, a complete new vascular tissue was formed. The exception was elastin, which was not detected either after patch implantation into the rat aorta or after patch implantation into sheep carotid arteries. Nevertheless, incorporated VEGF promoted harmonization of tissue formation processes in situ without signs of chronic granulomatous inflammation, neointimal hyperplasia, and calcification.

Immunofluorescence study of the explanted PHBV/PCL/RGD patches revealed the same structural ele-

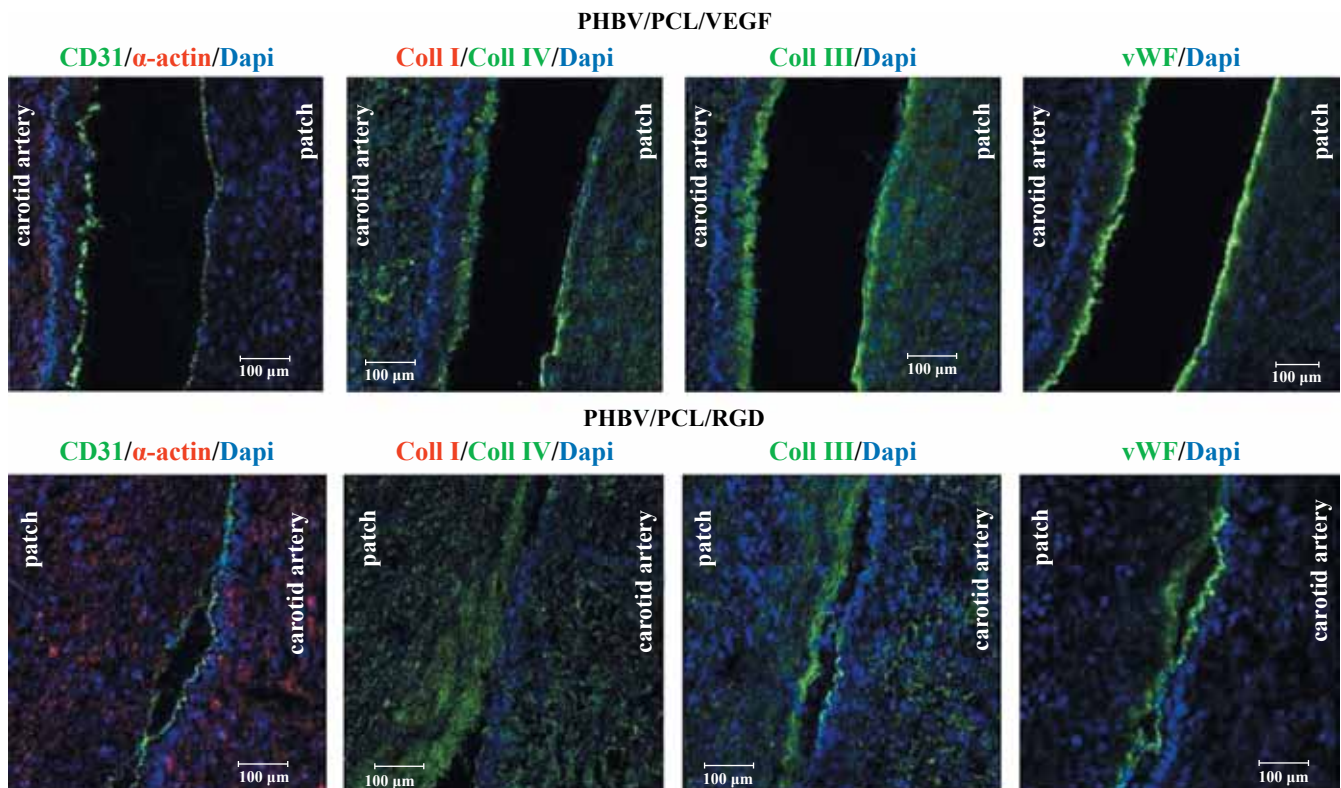


Fig. 4. Results of immunofluorescence study of explanted PHBV/PCL/VEGF and PHBV/PCL/RGD patches with surrounding sections of the sheep carotid artery: CD31/alpha actin/Dapi panel: mature endothelial cells (green glow), smooth muscle and other cells containing alpha actin (red glow); panel Coll I/Coll IV/Dapi: collagen type I (red glow), collagen type IV (green glow); Coll III/Dapi panel: collagen type III (green glow); vWF/Dapi panel: von Willebrand factor (green glow). The nuclei of all cells were stained with Dapi nuclear dye (blue glow). 100× magnification

ments of the new vascular tissue as in the PHBV/PCL/VEGF patches: endothelial monolayer consisting of CD31+vWF+ mature endothelial cells; type I, III and IV collagen (Figure 4). However, what draws attention is the higher number of smooth muscle cells in the neointima and high total cellularity of the patch wall due to the presence of chronic granulomatous inflammation, as well as the lower number of type III collagen relative to PHBV/PCL/VEGF patches (Fig. 4).

CONCLUSION

The efficacy of using pro-angiogenic growth factor VEGF and various configurations of RGD peptides, as well as different approaches to modifying the product, was evaluated in a comparative aspect in vitro and in preclinical tests on a sheep model.

The identified advantage of PHBV/PCL/VEGF biodegradable patches was that incorporation of VEGF into the patch during manufacturing by emulsion electrospinning and the absence of subsequent surface modification manipulations with aggressive surfactants resulted in preservation of physical and mechanical characteristics of the patches, without reducing strength and or increasing rigidity of the final product, as observed after modifying the surface of the biodegradable patches with RGD peptides. The hemocompatibility of PHBV/PCL/VEGF patches proved to be the highest even in comparison with the xeno-pericardial flap that is actively used in the clinic.

In the sheep model, patches with RGD, regardless of the peptide configuration, promoted endothelialization, but provoked neointimal hyperplasia and granulomatous inflammation, whereas the PHBV/PCL/VEGF patches in the sheep model demonstrated optimal ability to form a healthy new vascular tissue on their basis, with the formation of thin neointima lined with endothelium, middle smooth muscle layer and adventitia containing all the basic structural elements characteristic of this layer: bundles of collagen fibers, fibroblast-like cells and vasa vasorum. All this testifies to the high efficiency of the vascular endothelial growth factor incorporated into patches.

The research was carried out within the framework of the fundamental theme No. 0419-2022-0001 of the Research Institute for Complex Issues of Cardiovascular Diseases "Molecular, cellular and biomechanical mechanisms of pathogenesis of cardiovascular diseases in the development of new methods of treatment of cardiovascular diseases based on personalized pharmacotherapy, introduction of minimally invasive medical devices, biomaterials and tissue-engineered implants".

The authors declare no conflict of interest.

REFERENCES

1. Bonati LH, Dobson J, Featherstone RL, Ederle J, van der Worp HB, de Borst GJ, Mali et al. Long-term outcomes after stenting versus endarterectomy for treatment of symptomatic carotid stenosis: the international carotid stenting study (ICSS) randomised trial. *Lancet*. 2015; 385: 529–38. doi: 10.1016/S0140-6736(14)61184-3. PMID: 25453443.
2. Abbott AL, Paraskevas KI, Kakkos SK, Golledge J, Eckstein HH, Diaz-Sandoval LJ et al. Systematic review of guidelines for the management of asymptomatic and symptomatic carotid stenosis. *Stroke*. 2015; 46: 3288–3301. doi: 10.1161/strokeaha.115.003390. PMID: 26451020.
3. Gavrilenko AV, Kuklin AV, Fomina VV. Conventional and eversion carotid endarterectomy for internal carotid artery stenosis. *Pirogov Russian Journal of Surgery = Khirurgiya. Zurnal im. N.I. Pirogova*. 2018; (2): 87–92. [In Russ]. doi: 10.17116/hirurgia2018287-92.
4. Zannetti S, Cao P, De Rango P, Giordano G, Parlani G, Lenti M et al. Intraoperative assessment of technical perfection in carotid endarterectomy: a prospective analysis of 1305 completion procedures. Collaborators of the EVEREST study group. Eversion versus standard carotid endarterectomy. *Eur J Vasc Endovasc Surg*. 1999; 18 (1): 52–8. doi: 10.1053/ejvs.1999.0856. PMID: 10388640.
5. Ren S, Li X, Wen J, Zhang W, Liu P. Systematic review of randomized controlled trials of different types of patch materials during carotid endarterectomy. *PLoS one*. 2013; 8 (1): e55050. PMID: 23383053. doi: 10.1371/journal.pone.0055050.
6. Texakalidis P, Giannopoulos S, Charisis N, Giannopoulos S, Karasavvidis T, Koullias G et al. A meta-analysis of randomized trials comparing bovine pericardium and other patch materials for carotid endarterectomy. *J Vasc Surg*. 2018; 68 (4): 1241–1256. doi: 10.1016/j.jvs.2018.07.023. PMID: 30244928.
7. Karpenko AA, Kuzhuget RA, Starodubtsev VB, Ignatenko PV, Kim IN, Gorbatykh VN. Immediate and long-term outcomes of carotid bifurcation remodeling. *Patologiya krovoobrashcheniya i kardiokhirurgiya*. 2013; 17 (1): 21–24. [In Russ]. doi: 10.21688/1681-3472-2013-1-21-24.
8. Antonova LV, Sevostyanova VV, Mironov AV, Krivkina EO, Velikanova EA, Matveeva VG et al. In situ vascular tissue remodeling using biodegradable tubular scaffolds with incorporated growth factors and chemo-attractant molecules. *Complex Issues of Cardiovascular Diseases*. 2018; 7 (2): 25–36. doi: 10.17802/2306-1278-2018-7-2-25-36.
9. Smith RJ, Yi T, Nasiri B, Breuer CK, Andreadis ST. Implantation of VEGF-functionalized cell-free vascular grafts: regenerative and immunological response. *The FASEB Journal*. 2019; 33 (4): 5089–5100. doi: 10.1096/fj.201801856R.
10. Krilleke D, Ng YS, Shima DT. The heparin-binding domain confers diverse functions of VEGF-A in development and disease: A structure-function study. *Biochemi-*

- cal Society Transactions*. 2009; 37 (6): 1201–1206. doi: 10.1530/JOE-15-0342. PMID: 19909247.
11. Miyazu K, Kawahara D, Ohtake H, Watanabe G, Matsu-da T. Luminal surface design of electrospun small-diameter graft aiming at *in situ* capture of endothelial progenitor cell. *Journal of Biomedical Materials Research Part B: Applied Biomaterials*. 2010; 94 (1): 53–63. doi: 10.1002/jbm.b.31623.
 12. Wang F, Li Y, Shen Y, Wang A, Wang S, Xie T. The functions and applications of RGD in tumor therapy and tissue engineering. *International Journal of Molecular Sciences*. 2013; 14 (7): 13447–1362. doi: 10.3390/ijms140713447. PMID: 23807504.
 13. Hsu SH, Chu WP, Lin YS, Chiang YL, Chen DC, Tsai CL. The effect of an RGD-containing fusion protein CBD-RGD in promoting cellular adhesion. *Journal of Biotechnology*. 2004; 111 (2): 143–150. doi: 10.1016/j.jbiotec.2004.03.014. PMID: 15219401.
 14. Sevostianova VV, Mironov AV, Antonova LV, Krivkina EO, Matveeva VG, Velikanova EA et al. Tissue-engineered patch modified by vascular endothelial growth factor for reconstruction of vascular wall. *Patologiya krovoob-rashcheniya i kardiokirurgiya = Circulation Pathology and Cardiac Surgery*. 2020; 24 (4): 114–128. [In Russ]. doi: 10.21688/1681-3472-2020-4-114-128.
 15. Antonova LV, Silnikov VN, Khanova MYu, Koroleva LS, Serpokrilova IYu, Velikanova EA et al. Adhesion, proliferation and viability of human umbilical vein endothelial cells cultured on the surface of biodegradable non-woven matrices modified with RGD peptides. *Russian Journal of Transplantation and Artificial Organs*. 2019; 21 (1): 142–152. [In Russ]. doi: 10.15825/1995-1191-2019-1-142-152.
 16. Sevostianova VV, Antonova LV, Mironov AV, Yuzhalin AE, Silnikov VN, Glushkova TV et al. Biodegradable patches for arterial reconstruction modified with RGD peptides: results of an experimental study. *ACS Omega*. 2020; 5 (34): 21700–21711. doi: 10.1021/acsomega.0c02593. PMID: 32905385.
 17. Lin HB, Sun W, Mosher DF, Garciaecheverria C, Schaufelberger K, Lelkes PI et al. Synthesis, Surface, and Cell Adhesion Properties of Polyurethanes Containing Covalently Grafted RGD-peptides. *J Biomed Mater Res*. 1994; 28 (3): 329–342. doi: 10.1002/jbm.820280307. PMID: 8077248.
 18. Sedaghati T, Jell G, Seifalian A. Investigation of Schwann cell behaviour on RGD-functionalised bioabsorbable nanocomposite for peripheral nerve regeneration. *New Biotechnology*. 2014; 31 (3): 203–213. doi: 10.1016/j.nbt.2014.01.002. PMID: 24503165.
 19. Antonova LV, Mironov AV, Silnikov VN, Glushkova TV, Krivkina EO, Akent'eva TN et al. Biodegradable vascular patches: comparative characteristics of physical-mechanical and hemocompatible properties. *Yakut Medical Journal*. 2019; 4 (68): 35–39. doi: 10.25789/YMJ.2019.68.08.
 20. Wei K, Li Y, Mugishima H, Teramoto A, Abe K. Fabrication of core-sheath structured fibers for model drug release and tissue engineering by emulsion electrospinning. *Biotechnology Journal*. 2012; 7 (5): 677–685. doi: 10.1002/biot.201000473. PMID: 22125296.
 21. Spano F, Quarta A, Martelli C, Ottobrini L, Rossi RM, Giglic G et al. Fibrous scaffolds fabricated by emulsion electrospinning: from hosting capacity to *in vivo* biocompatibility. *Nanoscale*. 2016; 8 (17): 9293–9303. doi: 10.1039/C6NR00782A.
 22. Yarin R.L. Coaxial electrospinning and emulsion electrospinning of core-shell fibers. *Polymers for Advanced Technologies*. 2011; 22 (3): 310–317. doi: 10.1002/pat.1781.
 23. Ward AS, Cormier JM. Operative techniques in arterial surgery Dordrecht: Springer Netherlands. 1986.
 24. Hersel U, Dahmen C, Kessler H. RGD modified polymers: biomaterials for stimulated cell adhesion and beyond. *Biomaterials*. 2003; 24 (24): 4385–4415. doi: 10.1016/S0142-9612(03)00343-0. PMID: 12922151.
 25. Jolee Bartrom BS. ASTM Hemolysis. *NAMSA*. 2008; 1–12.
 26. Malm CJ, Risberg B, Bodin A, Bäckdahl H, Johansson BR, Gatenholm P et al. Small calibre biosynthetic bacterial cellulose blood vessels: 13-months patency in a sheep model. *Scand Cardiovasc J*. 2012; 46 (1): 57–62. doi: 10.3109/14017431.2011.623788. PMID: 22029845.
 27. Ahmed M, Hamilton G, Seifalian AM. The performance of a small-calibre graft for vascular reconstructions in a senescent sheep model. *Biomaterials*. 2014; 35 (33): 9033–9040. doi: 10.1016/j.biomaterials.2014.07.008. PMID: 25106769.
 28. Thomas LV, Lekshmi V, Nair PD. Tissue engineered vascular grafts – preclinical aspects. *Int J Cardiol*. 2013; 167 (4): 1091–1100. PMID: 23040078. doi: 10.1016/j.ijcard.2012.09.069.
 29. Swartz DD, Andreadis ST. Animal models for vascular tissue-engineering. *Curr Opin Biotechnol*. 2013; 24 (5): 916–925. doi: 10.1016/j.copbio.2013.05.005. PMID: 23769861.
 30. Hoerstrup SP, Cummings Mrcs I, Lachat M, Schoen FJ, Jenni R, Leschka S et al. Functional growth in tissue-engineered living, vascular grafts: follow-up at 100 weeks in a large animal model. *Circulation*. 2006; 114 (1 Suppl): I159–I166. doi: 10.1161/circulationaha.105.001172. PMID: 16820566.
 31. Catto V, Fare S, Freddi G, Tanzi MC. Vascular tissue engineering: recent advances in small diameter blood vessel regeneration. *ISRN Vasc Med*. 2014; 923030. doi: 10.1155/2014/923030.
 32. Matsuzaki Yu, Iwaki R, Reinhardt JW, Chang Yu-C, Miyamoto S, Kelly J et al. The effect of pore diameter on neo-tissue formation in electrospun biodegradable tissue-engineered arterial grafts in a large animal model. *Acta Biomater*. 2020; 115: 176–184. doi: 10.1016/j.actbio.2020.08.011. PMID: 32822820.
 33. Matsuzaki Yu, Miyamoto S, Miyachi H, Iwaki R, Shoji T, Blum K et al. Improvement of a Novel Small-diameter Tissue-engineered Arterial Graft With Heparin Conjugation. *Ann. Thorac. Surg*. 2021; 111 (4): 1234–1241. doi: 10.1016/j.actbio.2020.08.011. PMID: 32822820.

The article was submitted to the journal on 02.06.2022